Different Time-Frequency Distribution Patterns of Somatosensory Evoked Potentials in Dual- and Single-Level Spinal Cord Compression

Hongyan Cui, Yazhou Wang, Guangsheng Li, Yongcan Huang, and Yong Hu, *Senior Member, IEEE*

***Abstract*— Among patients with cervical myelopathy, the most common level of stenosis at spinal cord of all ages was reported to be between cervical levels C5-6. Previous studies found that time-frequency components (TFCs) of somatosensory evoked potentials (SEPs) possess location information of spinal cord injury (SCI) in single-level deficits in the spinal cord. However, the clinical reality is that there are multiple compressions at multiple spinal cord segments. This study proposed a new algorithm to differentiate distribution patterns of SEP TFCs between the dual-level compression and the corresponding single-level compression, which is potential in providing precise diagnosis of cervical myelopathy. In the present animal study, a group of rats with dual-level compressive (C5+6) injury to cervical spinal cord was investigated. SEPs were collected at 2 weeks after surgery, while SEP TFCs were calculated. The SEP TFCs under dual-level compression were compared to an existent dataset with one sham control group and three single level compression groups at C4, C5, C6. Behavioral evaluation showed very similar scale of injury severity between individual rats, while histology evaluation confirmed the precise location of injury. According to time-frequency distribution patterns, it showed that the middle-energy components of dual-level showed similar patterns as that of each single-level group. In addition, the low-energy components of the dual-level C5+6 group had the highest correlation with C5 ($R = 0.3423$, $p < 0.01$) and C6 ($R = 0.4000$, $p < 0.01$) groups, but much lower with C4 group ($R = 0.1071$, $p = 0.012$). These results indicated that SEP TFCs components possess information regarding the location of neurological lesion after spinal cord compression. It preliminarily demonstrated that SEP TFCs are likely a useful measure to provide location information of neurological lesions after compression SCI.**

***Index Terms*— Cervical myelopathy, chronic compression, spinal cord injury, somatosensory evoked potentials, time-frequency distribution, time-frequency components.**

I. Introduction

SOMATOSENSORY evoked potentials (SEPs) are commonly used for monitoring the functional integrity of the spinal cord during spine surgery [1]–[6]. In clinical practice, intraoperative SEPs can identify changes in spinal cord function prior to irreversible damage without providing any information about the exact location of the functional abnormality [7]. If the location of functional changes can be ascertained immediately, it would help the surgeon to prevent real spinal cord injury (SCI) by taking prompt and accurate action. Another clinical use of SEPs is to evaluate the neurological function in patients with spinal disorders, such as cervical myelopathy [8]–[13]. In clinical practice, the myelopathic level is commonly happened at C4 to C6 cervical spinal levels. The previous publications have reported that the myelopathy is appeared at C5-6 with high incidence [10], [14], [15], followed by C4-5 and C6-7. Nevertheless, after multi-level compression of the spinal cord, a precise diagnosis of which spinal cord levels are myelopathy would be beneficial when planning the necessary surgery [16]. However, it is still difficult to precisely identify the myelopathy location in a multi-level cervical stenosis.

Some studies have suggested the value of time–frequency analysis in detecting spinal cord injury [7], [17]. Unlike conventional measures of SEP using amplitude and latency, the location of SCI was correlated with changes in time-frequency components of the SEP. Previous studies proposed that the SEP signal could be decomposed into a series of time-frequency components (TFCs) that reflected the

Manuscript received November 12, 2021; revised March 19, 2022; accepted April 6, 2022. Date of publication April 13, 2022; date of current version April 25, 2022. This work was supported in part by the National Natural Science Foundation of China under Grant 81871768; in part by the Natural Science Foundation of Guangdong Province under Grant 2018A0303130105; and in part by the High Level-Hospital Program, Health Commission of Guangdong Province under Grant HKUSZH201902011. *(Corresponding author: Yong Hu.)*

Hongyan Cui is with the Institute of Biomedical Engineering, Chinese Academy of Medical Sciences and Peking Union Medical College, Tianjin 300192, China (e-mail: cokey1981@hotmail.com).

Yazhou Wang is with the Department of Orthopaedics and Traumatology, The Hong Kong University Shenzhen Hospital, Shenzhen, Guangdong 518053, China (e-mail: contemplativecat@gmail.com).

Guangsheng Li is with the Department of Orthopaedics and Traumatology, The Hong Kong University Shenzhen Hospital, Shenzhen, Guangdong 518053, China, and also with the Spinal Division, Department of Orthopaedics, Affiliated Hospital of Guangdong Medical University, Zhanjiang, Guangdong 524001, China (e-mail: guangshenglee@163.com).

Yongcan Huang is with the Shenzhen Engineering Laboratory of Orthopaedic Regenerative Technologies, Orthopaedic Research Center, Peking University Shenzhen Hospital, Shenzhen 518036, China (e-mail: hycpku@hotmail.com).

Yong Hu is with the Institute of Biomedical Engineering, Chinese Academy of Medical Sciences and Peking Union Medical College, Tianjin 300192, China, also with the Department of Orthopaedics and Traumatology, The Hong Kong University Shenzhen Hospital, Shenzhen, Guangdong 518053, China, and also with the Spinal Division, Department of Orthopaedics, Affiliated Hospital of Guangdong Medical University, Zhanjiang, Guangdong 524001, China (e-mail: yhud@hku.hk).

Digital Object Identifier 10.1109/TNSRE.2022.3167260

physiological mechanisms of nervous system function [18]–[22]. TFCs are a decomposition to explore peaks and components of SEP waveforms, which were reported with physiological origins of neural signals [23]–[27]. Two previous studies demonstrated that changes in distribution pattern of these SEP TFCs were associated with the locational difference of neurological lesions following SCI and these location-related patterns were stable across different injury modalities (acute and chronic) [21], [22]. These findings prompt the hypothesis that the SEP TFCs are able to provide location information of neurological lesion within the spinal cord, and if so, the alternation of SEP TFCs would be associated with the site of neurological lesion caused by chronic compression SCI. The above previous studies demonstrated the feasibility of SEP TFC pattern in identifying single-level deficits in the spinal cord. However, the clinical reality is that there are multiple compressions at multiple spinal cord segments [10], [15]. It is necessary to explore the relationship between the dual-level compression and the corresponding single-level compression. If there is information about the location of neurological lesion in TFC pattern, whether those TFCs of dual-level compression represent a combination of, or be closely related to, the patterns of the constituent single levels, which thereby infers that the dual-level pattern may be obtained using the patterns of its constituent single levels by regression methods.

In this study, we selected C4, C5 and C6 as single level compression model and C5-6 as dual-level compression model. The aim was to explore the potential values of SEP TFCs in indicating the location-related changes of neurological lesion following chronic compression SCI, and SEP TFC pattern after dual-level compression (at C5+6) was compared to that after each single-level compression (at C4, C5, or C6), and whether those TFCs in dual-level compression are measured in two single levels.

II. Material and Methods

In this section, the material and methods are stated, including the data source from animal model that is used, and the method for time-frequency analysis and statistical analysis of SEP signals.

A. Animal Model of Chronic Compressive SCI

Twelve adult Sprague-Dawley rats (weighing between 250 and 300 g) were administered with water-absorbing polymer implantation within the spinal canal over C5 and C6 two levels. SEP signals were collected in two weeks after surgical implantation. Higher resolution time-frequency analysis was applied on recorded SEP to produce TFCs under dual-level compression of C5+6. The experimental protocol and signal processing are similar as the previous study of single-level spinal cord compressive injury [20]. This study combined the data from a group of 12 rats underwent C5 and C6 dual-level compression with previous dataset from 4 groups of rats with single-level spinal cord compressive injury and sham control with normal neurological function (n = 12 per group) [20]. Based on the location of implantation within the spinal canal, the compression groups were termed the C4 group, C5 group, C6 group, and the C5+6 group. There is no difference on basic characteristics like weight and age of rats among five groups.

All experimental procedures were conducted in strict compliance with the institutional guidelines for the care and use of laboratory animals approved by the Committee on the Use of Live Animals in Teaching and Research of Li Ka Shing Faculty of Medicine of the University of Hong Kong (No. CULART 2912-12). Under general anesthesia maintained with 1.5% isoflurane, the surgery was performed following a well-established protocol to produce spinal cord compression using implantation of water-absorbing polymer [20]. In brief, after laminae C3-C7 were exposed through a posterior approach, the yellow ligament between the laminae was removed. The dura underneath was carefully separated from the laminae to prevent leakage of cerebrospinal fluid. The compression material is made of a water-absorbing polymer [20], which cross section is a standard square of 1 mm^2. The compression sheet was inserted between laminae of C5 and C6 and the dura. In single-level groups, the polymer compressor was placed on C4, C5 and C6 separately [20]. The polymer expands after implantation by absorbing tissue fluid, which produces chronic compression on the spinal cord in 2 hours after implantation. After surgery, the wound was closed by layers. The rats were kept on a warm electric blanket for thoroughly reviving. Then, each rat was allocated into cage individually and allowed free access for water and food. Rats with compressive injury were hosted for 2 weeks. Several previous studies had proved the safety of the polymer compressor without tissue granulation or inflammatory reaction after implantation [20]–[22], [28]. The location of pathological changes caused by compressive SCI was verified by haematoxylin-eosin (H&E) staining for histological evaluations.

The neurological deficit was evaluated by Basso, Beattie, and Bresnahan (BBB) locomotor rating scale [29]. The BBB scale is ranged from complete neurological function loss (score 0) to normal neurological function (score 21). Animals in this study were measured with BBB score at the time points of pre-injury, 1 week and 2 weeks after compression injury.

B. Somatosensory Evoked Potentials (SEP) Evaluation

Two weeks post-surgery, SEPs were collected from each rat anesthetized with 1.5% isoflurane. The SEPs were elicited by constant current stimuli delivered to the forepaw with a rate of 4.1 Hz that could avoid linear interference [30]. The stimuli intensities were twice the motor threshold. Cortical SEPs were recorded from the skull over the sensory cortex. The SEPs were amplified 5000 times at 10-2000 Hz (Zhuhai Yiruikeji Co., Ltd., China). Two hundred responses were averaged for each waveform to ensure the quality of the SEP signals with a SNR about 5-10 Hz.

For high-resolution time-frequency decomposition, a matching pursuit (MP) algorithm was employed to identify the time-frequency components (TFCs) within the averaged SEP waveform [19]. The MP algorithm is advantageous in that it can process non-stationary signals with heavy background

noise and can provide an adaptive approximation of the target signal with higher resolution than conventional time-frequency analysis methods [19, 31].

The MP algorithm decomposes an input signal $s(t)$ into a series of basic time-frequency components from a large redundant dictionary as follows:

$$s(t) = \sum_{m=0}^{M-1} c_m(t) + r(t) \tag{1}$$

where $c_m(t)$ is the m-th decomposed time-frequency component, m is the decomposition level, and $r(t)$ is the decomposition residue. Each component $c_m(t)$ is in a form specified by the time-frequency dictionary and is described by a set of parameters/features. A commonly-used time-frequency dictionary is the Gabor functions as follows:

$$c_m(t) = ae^{-\pi[(t-\tau)/\sigma]^2} cos(2\pi f(t-\tau) + \emptyset) \tag{2}$$

where τ, f, a, σ and φ define the latency, frequency, amplitude, span, and phase of $c_m(t)$, respectively. The features for each component will be concentrated resulting in a high-dimensional feature set for the following procedures.

All decomposed TFCs were classified into three categories based on their relative energy to facilitate the efficiency of classification [19]. Firstly, the high-energy TFC was defined as the component with the highest energy. Secondly, after selecting the high-energy TFC, other TFCs with relative energy greater than 2% were defined as 'middle-energy TFCs', and lastly the remaining TFCs below 2% were defined as 'low-energy TFCs'. In each group, TFCs with appearance in more than 60% were considered as stable components to be included in following study.

The distribution patterns of the decomposed TFCs were described by a joint probability density function (PDF), which was calculated by the conventional kernel density estimation using a Gaussian kernel [32]. These patterns were compared with each other, and the correlation coefficients between each pair of groups were calculated as follows:

$$r = \frac{\sum_m \sum_n (A_{mn} - \bar{A})(B_{mn} - \bar{B})}{\sqrt{\sum_m \sum_n (A_{mn} - \bar{A})^2 \sum_m \sum_n (B_{mn} - \bar{B})^2}} \tag{3}$$

where A and B are the 2-D matrix of distribution pattern, $\bar{A}$ and $\bar{B}$ are the mean values of A and B, respectively.

C. Statistical Analysis

All statistical analyses were performed with the software program SPSS 16.0 (SPSS Inc., Chicago, IL). Differences in BBB score among injury groups and in SEPs among groups were analyzed by one-way analysis of variance (ANOVA). The correlation of the low-energy SEP TFCs between the C4, C5, C6, and C5+6 groups was analyzed using Pearson correlation coefficient using bilateral, paired Student t-tests (two-tailed). It was designated at $\alpha = 0.05$. Generally, based on the absolute value of correlation coefficient, there is no correlation when the correlation coefficient is between 0-0.09, a weak correlation between 0.1-0.3, a moderate correlation between 0.3-0.5, and a strong correlation between 0.5-1.0. In practice, we judge the strength mainly by significance, not only by correlation coefficient itself. We also need to test whether the two groups of data are significantly correlated according to significant difference test result of P value. In neuroscience researches, the correlation coefficient of 0.3 is acceptable [30], [33]. In this study, it was considered a significant correlation when a p-value < 0.05 and an absolute correlation coefficient $R \geq 0.30$ (moderate or strong relationship) were observed.

TABLE I
FUNCTIONAL EVALUATION BY BASSO, BEATTIE, AND BRESNAHAN SCALE

BBB score	Pre-injury	1 week after injury	2 weeks after injury
Group C4	21	16.5±0.80	16.3±0.78
Group C5	21	16.4±0.79	16.1±0.83
Group C6	21	16.1±0.79	15.8±0.72
Group C5+6	21	16.2±0.83	15.8±0.75
ANOVA analysis		F=0.62, p=0.623	F=1.21, p=0.320
Average	21	16.3±0.80	16.0±0.79

III. EXPERIMENTS

In this section, we compare the time-frequency distribution patterns of the SEPs from dataset of animal SCI. Combining with the behavioral and histology evaluation, the details results are provided as follows.

A. Behavioral and Histology Evaluation

All rats before surgery were tested with full BBB score without any exception. Before surgery, the BBB scores were 21 points for all groups. After surgery, the BBB scores were 21 points for the sham group. However, for the injury groups after the compression injury, the neurological function in terms of BBB scale were measured in slight decrease as 16.3±0.80 in 1 week after injury and 16.0±0.79 in 2 weeks after injury. TABLE I showed the results of functional evaluation in different injury groups. There is no significant difference among 4 groups in either 1 week after injury ($p = 0.623$) or 2 weeks after injury ($p = 0.320$). Two weeks after injury, the pathological changes inside the spinal cord were observed by qualitative histology observation on H&E staining (Fig. 1 and Fig. 2). The gradually expanded polyurethane sheet induced an evident compression to the posterolateral spinal cord after absorbed water inside the spinal canal and resulted in spinal canal encroachment. The encroachment caused serious sunken deformation with a dented appearance on the dorsal or dorsal-lateral side of spinal cord and tissue loss in the compressive level of cord, but without obvious tissue edema and haemorrhage. In normal spinal cord, grey matter (butterfly-like shape) and surrounded white matter with organized neural fiber structure can be clearly identified. While, in the compression level of the cord, such anatomic morphology and structure was seriously destroyed. Serious deformation of white matter even with grey matter was found on the posterolateral funiculus

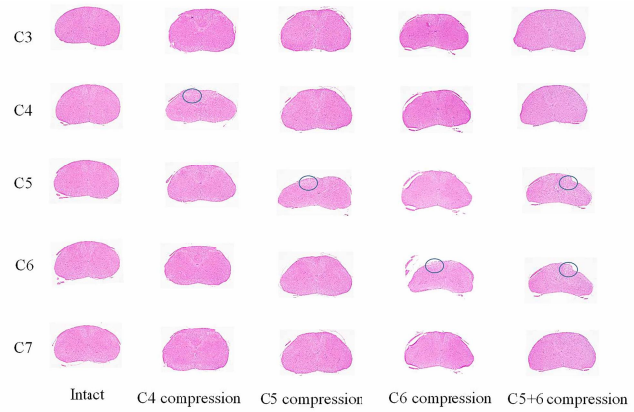

Fig. 1. Histological evaluations of normal and injury cord by H&E staining.

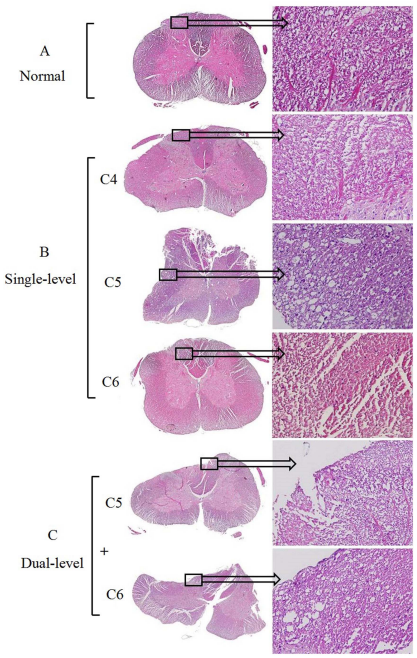

Fig. 2. Histological evaluations of each group by H&E staining.

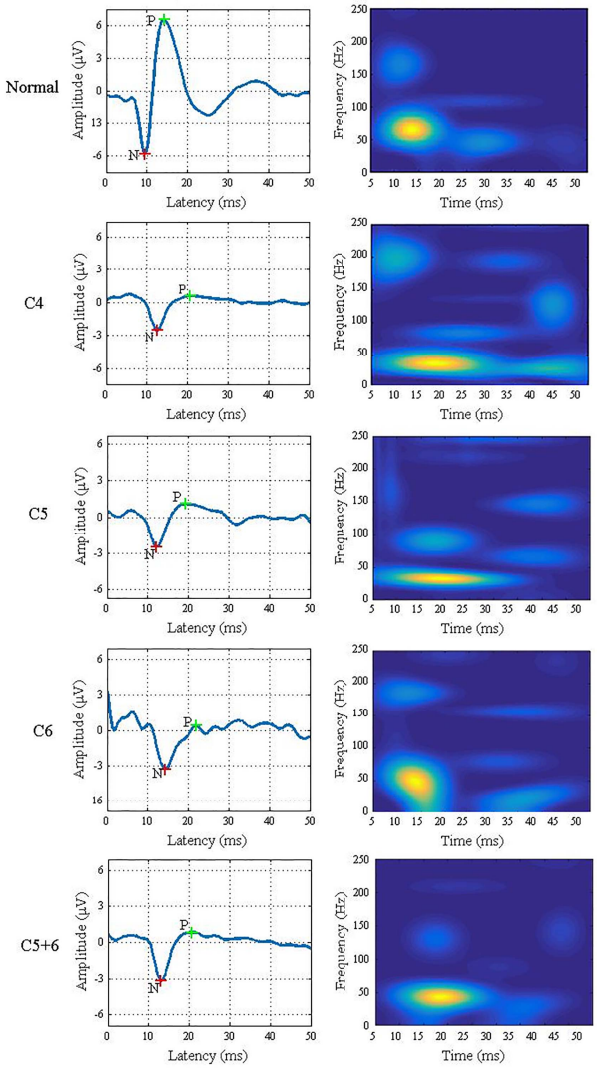

Fig. 3. SEP waveforms and time-frequency distributions.

of the compressive level. Disorganization of neural fibers and vacuolation of posterolateral funiculus tissue were seen on the compressive region. In addition, no structural changes of the spinal cord in the adjacent segments were found (Fig. 1). Thus, histology evaluation confirmed the precise location of injury, while results from behavioral evaluation showed very limit variability of dysfunction between individual rats.

B. SEP Waveforms and Time-Frequency Distribution Patterns

Figure 3 is a representative example SEP waveforms and time-frequency distributions from each group. Each row represented averaging signals and the corresponding time-frequency maps of the normal group and the various SCI groups. In the time domain (first column in Fig. 3), there was a dominant SEP wave in each group. But two weeks post-surgery, the results showed that the amplitudes are decreased significantly and the latencies are delayed significantly in injury groups compared to normal group ($p < 0.05$, TABLE II), which were reported in a previous article [20]. In addition, there were no significant statistical differences on the changes between the four injury groups ($p > 0.05$). These results proved there were spinal cord damages in the injury groups.

TABLE II
THE VALUES OF LATENCY AND AMPLITUDE OF EACH GROUP

Groups	Latency (ms)	Changes (%)	Amplitude (μV)	Changes (%)
Normal	11.05 ± 0.90		6.62 ± 2.78	
C4	12.59 ± 0.84*	13.94	2.73 ± 1.63*	58.76
C5	12.17 ± 2.35*	10.14	2.18 ± 2.08*	67.82
C6	13.22 ± 1.69*	19.64	2.93 ± 1.60*	55.74
C5+6	12.80±2.45*	16.38	5.05±2.29*	58.46

* $p < 0.05$ indicates a significant statistical difference compared to the normal control group.

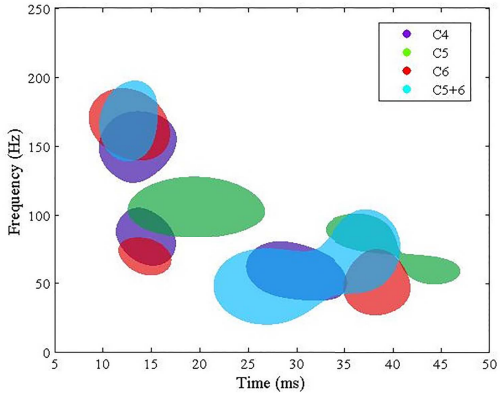

Fig. 4. Comparison of the distribution patterns of the middle-energy TFCs among different groups.

In the time-frequency domain, one dominant peak (high-energy component constructed by the main wave in the first column) was observed (second column in Fig. 3), accompanied by a series of smaller components (middle- and low-energy TFCs), the peak time and frequency determined the distribution patterns of the main SEP TFCs. Comparing with the normal group, the high-energy component after SCI showed decrease in peak energy, reduction in peak frequency and lengthen in peak time. Agreed with previous reports [20], [21], the high-energy component was found to be useful in reflecting whether an injury is present in the spinal cord. More importantly, obvious differences among different injury levels could be visualized in the SEP time-frequency distributions of the smaller components.

C. Comparison of Middle- and Low-Energy TFCs Among Different Groups

The time-frequency distribution patterns of middle- and low-energy components in the dual-level C5+6 group were compared with those of each single-level group. Results showed that middle-energy components of C5+6 group showed similar patterns as that of each single-level group (Fig. 4). Comparatively, low-energy components of C5+6 group had a number of overlapping/coupling areas with those in C5 and C6 group respectively (Fig. 5B), but had a distinct distribution pattern from that in the C4 group (Fig. 5A). Therefore, this particularly indicated the differences in low-energy TFCs among various injury groups.

D. Correlation Analysis of the Low-Energy TFCs Between Different Groups

The time-frequency distribution patterns of the low-energy SEP TFCs in the C5+6, C5, C6, and C4 levels and the correlation coefficients (with a confidence interval of 95%) between each pair were shown in Fig. 6. The pattern of the dual-level C5+6 group had the highest correlation with the C5 group ($R = 0.3423$, $p < 0.01$) and C6 group ($R = 0.4000$, $p < 0.01$), but a much lower correlation with the pattern of the C4 group ($R = 0.1071$, $p = 0.012$). For the remaining pairs, time-frequency patterns of the three single-level groups had significantly low correlation coefficient values between each other; correlation coefficients were all below 0.3 (C4 vs. C5: $R = 0.2276$, $p < 0.01$; C4 vs. C6: $R = 0.2064$, $p < 0.01$; C5 vs. C6: $R = 0.2356$, $p < 0.01$).

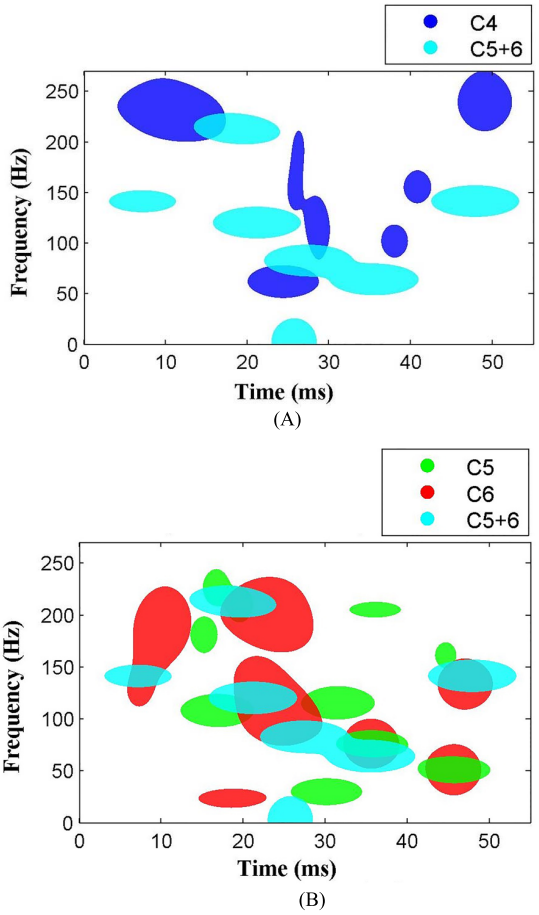

Fig. 5. Comparison of the distribution patterns of the low-energy TFCs among different groups. A: C5+6 group vs. C4 group; B: C5+6 group vs. C5 and C6 group.

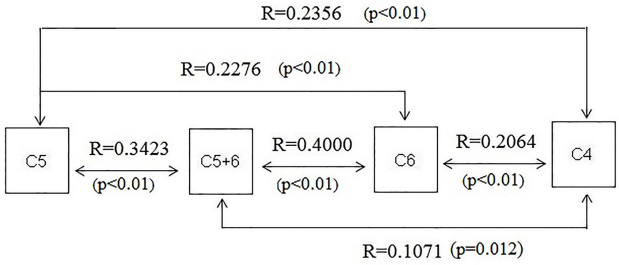

Fig. 6. Time-frequency patterns of the low-energy SEP TFCs of different compression groups and the correlation coefficients (R) between various pairs of them.

IV. Discussions

SEPs are electrical signals in the brain in response to external stimuli on the peripheral nerve [1]. The waveforms of SEP possess various components to reflect pathological changes along the sensory pathway from peripheral nerve to cortex. Analysis of SEP in TFCs would provide location information about functional deficits, which help clinicians

to make precise therapies [34]–[37]. Previous studies have reported that high-energy TFCs in SEPs based time-frequency domain could reflect the functional integrity of the spinal cord, and the smaller components may contain information regarding the location of neurological lesion after SCI at various single levels [20]–[22]. It is inspired to further verify the detail location information inside the SEP TFCs under the condition of dual-level neurological deficits of the spinal cord. In the present study, we examined the distribution pattern of SEP TFCs after chronic compression at dual levels, and compared the findings with single-level compressions. The findings in TFC pattern of dual-level (e.g., C5+6) neurological lesion were also observable in the condition involving the relative single levels (C5 or C6), and it could be distinct from the patterns of other irrelevant levels.

This study aimed to provide a neurological evaluation method for the early diagnosis of cervical myelopathy. In order to reproduce characteristic features of clinical cervical myelopathy in the early stages, a rat model of mild chronic compression was developed using a water-absorbing polyme. Compared with other types of spinal cord models, this compression model has the advantage that it is easier to control the site (level) of injury, and has been confirmed successful to produce chronic cervical cord compression previously [28], [38]–[42]. The histological evaluations showed that this animal model properly reproduces characteristic features of clinical myelopathy at the compressed levels where the expansion material was inserted, and were consistent with the BBB score results that the injury groups have a significant lower score about 16.

For SEP data collection, we utilized an established animal model of chronic compression injury to the cervical cord, and the severity of neurological deficits is mild in comparison with other models like contusion, displacement and transection spinal cord injury models [43]–[45]. In practice, the SEP signal can be elicited and transmitted along sensory nerves following stimulation of peripheral nerve fibers in the upper limb. The afferent signal travels up the dorsal column through the cervical segment of the spinal cord, and finally arrives at the brainstem and cerebral hemispheres [46]. The dorsal column pathways in the spinal cord are considered the primary sites that mediate the SEP components. Thus, various lesion sites along the spinal cord may influence the mediation effect and thereby lead to differing morphological changes of SEPs. With mild neurological deficits in this study, the pathological changes evaluated by H&E staining are located in the injury level of the cervical cord in two weeks after injury as reported in previous study [20], [28], [38], [40]–[42], [47], the results were consistent with other semi-quantitative or quantitative analysis methods like the LFB staining [28], [40], MRI [28], [30], [40], micro-CT [38], [41], it inferred that the injury took place in the condition of chronic spinal cord compression.

The analysis of SEP requires high quality of SEP signals. In practice, SEP signals are usually accompanied by noise from movement artifact, other electrophysiological signals, and environmental electromagnetic activity, which resulted in a low SNR (−20∼-30Hz) [48], and the ensemble-averaging method were commonly used to enhance the SNR, previous study obtained measurable SEP signals with 100 to 500 trials to be averaged [11]. In order to retain small components, we averaged 200 times to obtain a measurable SEP with a good SNR about 5-10 Hz. For better to quantify any changes corresponding to the spinal cord injury, the amplitude and latency of the main SEP waveforms were usually detected [11]–[13]. The SEP latency is a measure of signal transmission time along the somatosensory pathway (from peripheral nerves to the brain), and suggested to be more informative than the amplitude to reflect the integrity of the spinal cord [13]. In the present study, in order to retain small components, we averaged 200 times to obtain a measurable SEP with a good SNR about 5-10 Hz, and got typical SEP waveforms of the normal and each injury group with different latencies, that the peak latencies were a few milliseconds earlier in the normal group, were comparatively later in the injury groups, but it was hard to distinguish the injury groups according to changes of the latency in time-domain. Therefore, we analyzed SEP in time-frequency domain. Injuries at different locations within the dorsal column had been previously reported to produce different SEP patterns in the time-frequency domain [20]–[22]. In this study, we compared the distribution patterns of SEP TFCs in three energy scales measured by PDF. We further found that the distribution changes of SEP TFCs can reflect changes in deficit sites along the cervical cord. In the SEP waveform, this change in (low-energy) TFCs corresponds to the alteration of small fluctuations superimposed on the main wave, which reflects the locational difference of neurological lesions resulting from the spinal cord compression. This finding further proves that locational information about the cervical cord neurological lesions is contained in these TFCs.

Moreover, we found the evidence of an additive effect of a combination of pathological changes at two levels (C5+6) on the pattern of SEP TFCs, that the pattern of the C5+6 group had moderate correlation with the patterns of the individual C5 and C6 groups, while it had a weaker correlation with the pattern of the C4 group. It indicated that the pattern in C5+6 group was an approximate combination of the C5 group pattern and the C6 group pattern. These two single-level patterns have large areas coupled with the pattern of C5+6 group, with few unique areas distinguished from the C5+6 group pattern. The relationship between the dual-level C5+6 and its constituent single levels, C5 and C6, resulted in a correlation in the SEP TFC patterns between the groups. Our findings suggest that the TFCs in dual-level injury like C5+6 will probably be obtained from TFCs of two relevant single-levels (C5 and C6) using linear regression methods.

In clinical practice, a precise diagnosis of the deficit location following dual-level compression is difficult, since there is no consistent one-to-one correspondence between anatomical abnormalities and neurological impairment. In fact, the presence of abnormal cord anatomy can often be found without any impairment of neurological changes [8], [9]. Findings in this study provide a good deal of insight into the relationship between single- and dual-level neurological lesions and a potential method of identifying the offending level of functional abnormality after dual-level spinal cord compression. Recently, we have successfully recognized the cervical

myelopathy location from somatosensory evoked potentials using SEP TFCs of rat model [47]. Previous studies have reported that the TFCs components in rat SEPs are similar to those in humans [19]–[22], [47]–[50], suggesting this new time-frequency method may be translated to clinical use for identifying single or dual level neurological lesions in multi-level stenosis. In another study, we have reported translational findings regarding the relationships among SEP waveforms of rats and those of humans with normal neurology [51], showed that there were three stable TFC distribution regions in rat and human groups in the intact spinal cord condition, and there were significant correlations ($p < 0.05$) and linear relationships between the main SEP TFCs of human and rat groups by regression method. This shows the importance and potential application value of our present research.

The major contribution of this study is that has investigated the relationship of low-energy SEPs TFCs in each single-level and dual- level, and whether those TFCs in dual-level compression are measured in two single levels. It is a further proof of the location information inside TFCs. But there are several limitations to this study. The assessment of injury location is qualitative in this study, the precise relationship of SEP TFCs distribution among dual-level C5+6 and single-level C5 and C6 has not been determined, further quantitative histology analysis and immunohistochemistry test may provide precise assessment of the injury. In addition, it needs intensive study to explore the SEP TFCs features with more multi-level compressions. Because in many clinical cases, such as cervical myelopathy, the cervical spine degenerates at multiple locations, which results in multi-level neurological lesions [10], so further investigation will be conducted on SEP TFCs following SCI at other combination of levels (e.g., C4+5, C4+6, C4+5+6, C3+4+5+6, etc.), it would give concrete evidence to the usefulness of SEPs in location identification. Furthermore, this study focused on mild chronic compression. For serious injury, SEP waveforms are sometimes obscured by noise and may even vanish in some injuries. So, the identification of pathological location after other SCI grades of chronic compression (such as moderate and severe injury) and after other SCI types (such as displacement and local ischemia) is waiting for further studies. Besides, an important consideration is that clinical applicability of our results. It is important to show the entire spinal cord after injury, not only the responsible segments (compressed levels). The present study was designed as a pilot study to investigate the potential values of SEP TFCs in indicating the location-related changes of neurological lesion following chronic dual- and single-level spinal cord compression SCI. We performed H&E to assessment of injury at the adjacent levels next to the compressed levels with mild neurological deficits (Fig.1), the pathological changes were located in the injury level without developing to adjacent levels of the cervical cord in two weeks after injury, it is consistent with the vascular index (VI) by CD34 immunohistochemistry and microvessel density (MVD) measured by micro-CT quantification in two weeks after injury four in a previous study [38]. But in clinical practice, human chronic cord compression has shown multilevel myelopathy despite single level stenosis [15]. A previous experiment has also demonstrated the adjacent segments above or below compressed sites was also affected by the compression at postoperative 6 months. The reason for this result may be due to the observation period of time after compression, as we only observed at two weeks after a mild compression, it may affect only the responsible segment (compressed level) of the spinal cord. In clinical practice, many patients despite compression of the spinal cord, stay asymptomatic for months or years until they start to suffer from sensorimotor deficits caused by myelopathy. The potential role of this study based on time-frequency TFCs will help in clinical decision making (i.e., early surgery vs. conservative treatment) in the early diagnosis of the cervical myelopathy, and we have reported the preliminary translating findings to humans in a previous paper [51]. This study is a preliminary new discovery and observation, the model is the first to used at dual-level compression, it still needs study to provide more detailed information on mechanism exploration in further. To evaluate the potential efficacy of the SEP TFCs, further experiment should be conducted to better simulate the real situation of myelopathy in patient with single- and multi-level cervical spinal stenosis (contained adjacent segmental lesions), with long time after the compression symptoms, so as to discover more evidence to determine the exact injury in our future study. This will be developed, and would help surgeons to select the most appropriate treatment.

V. Conclusion

The SEP TFC pattern of neurological lesion caused by dual-level compression SCI (C5+6) was correlated with the TFC patterns of its constituent single-levels (C5 and C6), but is distinct from the TFC pattern of C4. A TFC pattern of dual-level compressive SCI could be assembled with relevant TFC patterns of the single-level SCI at the involved levels. These findings suggest that SEP TFCs are likely to possess information regarding the location of neurological lesion after spinal cord compression. It contributes to a finer understanding of SEP morphology and explores the relationship between SEP components with deficits locating, beyond its conventional application in detecting functional integrity. Additionally, it is possible to simulate the SEP pattern of neurological lesion caused by dual-level compressive SCI using regression analysis of single-level patterns.

References

[1] M. R. Nuwer *et al.*, "Evidence-based guideline update: Intraoperative spinal monitoring with somatosensory and transcranial electrical motor evoked potentials," *J. Clin. Neurophysiol.*, vol. 29, no. 1, pp. 101–108, 2012.

[2] M. R. Nuwer, "Spinal cord monitoring with somatosensory techniques," *J. Clin. Neurophysiol.*, vol. 15, no. 3, pp. 183–193, May 1998.

[3] R. D. Labrom, M. Hoskins, C. W. Reilly, S. J. Tredwell, and P. K. H. Wong, "Clinical usefulness of somatosensory evoked potentials for detection of brachial plexopathy secondary to malpositioning in scoliosis surgery," *Spine*, vol. 30, no. 18, pp. 2089–2093, Sep. 2005.

[4] G. Waterstraat, M. Scheuermann, and G. Curio, "Non-invasive single-trial detection of variable population spike responses in human somatosensory evoked potentials," *Clin. Neurophysiol.*, vol. 127, no. 3, pp. 1872–1878, Mar. 2016.

[5] P. D. Thirumala *et al.*, "Diagnostic accuracy of somatosensory evoked potentials in evaluating new neurological deficits after posterior cervical fusions," *Spine*, vol. 42, no. 7, pp. 490–496, 2017.

[6] J. W. Duncan, R. A. Bailey, and R. Baena, "Intraoperative decrease in amplitude of somatosensory-evoked potentials of the lower extremities with interbody fusion cage placement during lumbar fusion surgery," *Spine*, vol. 37, no. 20, pp. E1290–E1295, Sep. 2012.

[7] Y. Hu, "Application of time-frequency analysis to somatosensory evoked potential for intraoperative spinal cord monitoring," *J. Neurol. Neurosurgery Psychiatry*, vol. 74, no. 1, pp. 82–87, Jan. 2003.

[8] J. A. Kaiser and B. A. Holland, "Imaging of the cervical spine," *Spine*, vol. 23, no. 24, pp. 2701–2712, 1998.

[9] T. Kanchiku, T. Taguchi, K. Kaneko, Y. Fuchigami, H. Yonemura, and S. Kawai, "A correlation between magnetic resonance imaging and electrophysiological findings in cervical spondylotic myelopathy," *Spine*, vol. 26, no. 13, pp. E294–E299, Jul. 2001.

[10] J. A. Tracy and J. D. Bartleson, "Cervical spondylotic myelopathy," *Neurologist*, vol. 16, no. 3, pp. 176–187, 2010.

[11] Y. Hu, Y. Ding, D. Ruan, Y. W. Wong, K. M. C. Cheung, and K. D. K. Luk, "Prognostic value of somatosensory-evoked potentials in the surgical management of cervical spondylotic myelopathy," *Spine*, vol. 33, no. 10, pp. E305–E310, May 2008.

[12] S. I. Nakai, M. Sonoo, and T. Shimizu, "Somatosensory evoked potentials (SEPs) for the evaluation of cervical spondylotic myelopathy: Utility of the onset-latency parameters," *Clin. Neurophysiol.*, vol. 119, no. 10, pp. 2396–2404, Oct. 2008.

[13] H. Cui, Y. Wang, X. Li, X. Xie, S. Xu, and Y. Hu, "Trial-to-trial latency variability of somatosensory evoked potentials as a prognostic indicator for surgical management of cervical spondylotic myelopathy," *J. Neuroeng. Rehabil.*, vol. 12, no. 1, p. 49, Dec. 2015.

[14] M. Matsumoto *et al.*, "MRI of cervical intervertebral disks in asymptomatic subjects," *J. Bone Joint Surg. Brit. Volume*, vol. 80, no. 1, pp. 19–24, 1998.

[15] K. Vallotton *et al.*, "Tracking white and gray matter degeneration along the spinal cord axis in degenerative cervical myelopathy," *J. Neurotrauma*, vol. 38, no. 21, pp. 2978–2987, Nov. 2021.

[16] H. Huang *et al.*, "Review of clinical neurorestorative strategies for spinal cord injury: Exploring history and latest progresses," *J. Neurorestoratol.*, vol. 1, no. 1, pp. 171–178, 2018.

[17] J. C. Braun, D. F. Hanley, and N. V. Thakor, "Detection of neurological injury using time-frequency analysis of the somatosensory evoked potential," *Electroencephalogr. Clin. Neurophysiol.*, vol. 100, no. 4, pp. 310–318, Jul. 1996.

[18] Z. Zhang, K. D. K. Luk, and Y. Hu, "Identification of detailed time-frequency components in somatosensory evoked potentials," *IEEE Trans. Neural Syst. Rehabil. Eng.*, vol. 18, no. 3, pp. 245–254, Jun. 2010.

[19] Z. G. Zhang, J. L. Yang, S. C. Chan, K. D. K. Luk, and Y. Hu, "Time-frequency component analysis of somatosensory evoked potentials in rats," *Biomed. Eng. OnLine*, vol. 8, no. 1, Dec. 2009.

[20] Y. Wang, G. Li, K. D. K. Luk, and Y. Hu, "Component analysis of somatosensory evoked potentials for identifying spinal cord injury location," *Sci. Rep.*, vol. 7, no. 1, p. 2351, Dec. 2017.

[21] Y. Wang, H. Cui, J. Pu, K. D. K. Luk, and Y. Hu, "Time-frequency patterns of somatosensory evoked potentials in predicting the location of spinal cord injury," *Neurosci. Lett.*, vol. 603, pp. 37–41, Aug. 2015.

[22] Y. Z. Wang *et al.*, "Usefulness of time-frequency patterns of somatosensory evoked potentials in identification of the location of spinal cord injury," *J. Clin. Neurophysiol.*, vol. 32, no. 4, pp. 341–345, 2015.

[23] T. R. Marra, "The origins of the subcortical component of the median nerve somatosensory evoked potentials," *Clin. Electroencephalogr.*, vol. 13, no. 2, pp. 116–121, Apr. 1982.

[24] F. Mauguière and J. Courjon, "The origins of short-latency somatosensory evoked potentials in humans," *Ann. Neurol.*, vol. 9, no. 6, pp. 607–611, Jun. 1981.

[25] T. Nakanishi, M. Tamaki, K. Arasaki, and N. Kudo, "Origins of the scalp-recorded somatosensory far field potentials in man and cat," *Electroencephalogr. Clin. Neurophysiol.*, vol. Suppl, 36, pp. 336–348, 1982.

[26] T. Nakanishi, M. Tamaki, Y. Ozaki, and K. Arasaki, "Origins of short latency somatosensory evoked potentials to median nerve stimulation," *Electroencephalogr. Clin. Neurophysiol.*, vol. 56, no. 1, pp. 74–85, Jul. 1983.

[27] K. Shimoji, M. Matsuki, and H. Shimizu, "Wave-form characteristics and spatial distribution of evoked spinal electrogram in man," *J. Neurosurg.*, vol. 46, no. 3, pp. 304–313, Mar. 1977.

[28] H. Q. Long *et al.*, "Is the speed of chronic compression an important factor for chronic spinal cord injury rat model?" *Neurosci. Lett.*, vol. 545, pp. 75–80, Jun. 2013.

[29] D. M. Basso, M. S. Beattie, and J. C. Bresnahan, "A sensitive and reliable locomotor rating scale for open field testing in rats," *J. Neurotrauma*, vol. 12, no. 1, pp. 11–21, 1995.

[30] K. D. K. Luk, Y. Hu, W. W. Lu, and Y. W. Wong, "Effect of stimulus pulse duration on intraoperative somatosensory evoked potential (SEP) monitoring," *J. Spinal Disorders*, vol. 14, no. 3, pp. 247–251, Jun. 2001.

[31] K. Schiecke, M. Wacker, F. Benninger, M. Feucht, L. Leistritz, and H. Witte, "Matching pursuit-based time-variant bispectral analysis and its application to biomedical signals," *IEEE Trans. Biomed. Eng.*, vol. 62, no. 8, pp. 1937–1948, Aug. 2015.

[32] O. D. Creutzfeldt, G. Bodenstein, and J. S. Barlow, "Computerized EEG pattern classification by adaptive segmentation and probability density function classification. Clinical evaluation," *Electroencephalogr. Clin. Neurophysiol.*, vol. 60, no. 5, pp. 373–393, May 1985.

[33] W. J. Levy, S. Levin, and B. Chance, "Near-infrared measurement of cerebral oxygenation. Correlation with electroencephalographic ischemia during ventricular fibrillation," *Anesthesiology*, vol. 83, no. 4, pp. 738–746, 1995.

[34] D. Telemacque *et al.*, "Method of decompression by durotomy and duroplasty for cervical spinal cord injury in patients without fracture or dislocation," *J. Neurorestoratol.*, vol. 6, no. 1, pp. 158–164, 2018.

[35] L. Chen, Y. Zhang, X. He, and S. Hooshang, "Comparison of intramedullary transplantation of olfactory ensheathing cell for patients with chronic complete spinal cord injury worldwide," *J. Neurorestoratol.*, vol. 1, no. 1, pp. 146–151, 2018.

[36] L. Chen, Y. Feng, Y. Zhang, H. Huang, and X. Guo, "Multicenter, randomized, double-blind placebo-control intramedullary decompression for acute complete spinal cord contusion injury," *J. Neurorestoratol.*, vol. 1, no. 1, pp. 165–170, 2018.

[37] G. A. Moviglia, M. T. Moviglia Brandolino, D. Couto, and S. Piccone, "Local immunomodulation and muscle progenitor cells induce recovery in atrophied muscles in spinal cord injury patients," *J. Neurorestoratol.*, vol. 1, no. 1, pp. 136–145, 2018.

[38] H. Q. Long, W. H. Xie, W. L. Chen, W. L. Xie, J. H. Xu, and Y. Hu, "Value of micro-CT for monitoring spinal microvascular changes after chronic spinal cord compression," *Int. J. Mol. Sci.*, vol. 15, no. 7, pp. 12061–12073, 2014.

[39] P. Kim, T. Haisa, T. Kawamoto, T. Kirino, and S. Wakai, "Delayed myelopathy induced by chronic compression in the rat spinal cord," *Ann. Neurol.*, vol. 55, pp. 503–511, 2004.

[40] X. Li, G. Li, K. D. K. Luk, and Y. Hu, "Neurorestoratology evidence in an animal model with cervical spondylotic myelopathy," *J. Neurorestoratol.*, vol. 5, pp. 21–29, Jan. 2017.

[41] Y. Hu, C. Y. Wen, T. H. Li, M. H. Cheung, X. K. Wu, and D. K. Luk, "Somatosensory-evoked potentials as an indicator for the extent of ultrastructural damage of the spinal cord after chronic compressive injuries in a rat model," *Clin. Neurophysiol.*, vol. 122, no. 7, pp. 1440–1447, 2011.

[42] S. Yamamoto, R. Kurokawa, and P. Kim, "Cilostazol, a selective type III phosphodiesterase inhibitor: Prevention of cervical myelopathy in a rat chronic compression model," *J. Neurosurg. Spine*, vol. 20, no. 1, pp. 93–101, 2014.

[43] D. D. Pearse *et al.*, "Histopathological and behavioral characterization of a novel cervical spinal cord displacement contusion injury in the rat," *J. Neurotrauma*, vol. 22, no. 6, pp. 680–702, Jun. 2005.

[44] N. S. S. Lau, C. A. Gorrie, J. Y. Chia, L. E. Bilston, and E. C. Clarke, "Severity of spinal cord injury in adult and infant rats after vertebral dislocation depends upon displacement but not speed," *J. Neurotrauma*, vol. 30, no. 15, pp. 1361–1373, Aug. 2013.

[45] A. Vipin *et al.*, "Natural progression of spinal cord transection injury and reorganization of neural pathways," *J. Neurotrauma*, vol. 33, no. 24, pp. 2191–2201, Dec. 2016.

[46] T. Yamada, M. Yeh, and J. Kimura, "Fundamental principles of somatosensory evoked potentials," *Phys. Med. Rehabil. Clin.*, vol. 15, no. 1, pp. 19–42, 2004.

[47] H. Cui, Y. Wang, G. Li, Y. Huang, and Y. Hu, "Exploration of cervical myelopathy location from somatosensory evoked potentials using random forests classification," *IEEE Trans. Neural Syst. Rehabil. Eng.*, vol. 27, no. 11, pp. 2254–2262, Nov. 2019.

[48] Y. Hu, H. Liu, and K. D. K. Luk, "Signal-to-noise ratio of intraoperative tibial nerve somatosensory-evoked potentials," *J. Clin. Neurophysiol.*, vol. 27, no. 1, pp. 30–33, 2010.

[49] M. A. Franceschini, I. Nissilä, W. Wu, S. G. Diamond, G. Bonmassar, and D. A. Boas, "Coupling between somatosensory evoked potentials and hemodynamic response in the rat," *NeuroImage*, vol. 41, no. 2, pp. 189–203, 2008.

[50] S. Di and D. S. Barth, "Topographic analysis of field potentials in rat vibrissa/barrel cortex," *Brain Res.*, vol. 546, no. 1, pp. 12–106, 1991.

[51] H. Y. Cui, Y. X. Wu, R. Li, G. S. Li, and Y. Hu, "A translational study of somatosensory evoked potential time-frequency components among rats, goats, and humans," *Neural Regener. Res.*, vol. 16, no. 11, pp. 2269–2275, 2021.